PERGAMON

International Journal of Heat and Mass Transfer 44 (2001) 4613–4623

International Journal of HEAT and MASS TRANSFER

www.elsevier.com/locate/ijhmt

Effect of inclination on the air-side performance of a brazed aluminum heat exchanger under dry and wet conditions

Man-Hoe Kim [a,*], Baek Youn [b], Clark W. Bullard [a]

[a] *Department of Mechanical and Industrial Engineering, University of Illinois at Urbana-Champaign, 1206 West Green Street, Urbana, IL 61801, USA*

[b] *Air-conditioner Development Group, Samsung Electronics Company, Maetan-3dong, Suwon 442-742, Republic of Korea*

Received 19 November 2000; received in revised form 8 March 2001

Abstract

This study presents the effect of an inclination angle from the vertical position on the air-side thermal hydraulic performance for a multi-louvered fin and flat tube heat exchanger. For a heat exchanger with a louver angle of 27°, fin pitch of 1.4 mm and flow depth of 20 mm, a series of tests for dry and wet surface conditions were conducted for the air-side Reynolds numbers of 100–300. The inclination angles from the vertical position were 0°, ±30°, ±45°, and ±60° clockwise. The heat transfer performance for both dry and wet conditions was neither influenced significantly by the inclination angle ($-60° < \theta < 60°$), nor by the presence or absence of an upstream duct, while the pressure drops increased consistently with the inclination angle. The heat transfer coefficients and the pressure drops for the wet conditions revealed the importance of the role of condensate drainage. © 2001 Published by Elsevier Science Ltd.

Keywords: Heat transfer enhancement; Heat exchanger; Inclination angle; *j*-factor; *f*-factor

1. Introduction

The effect of an inclination angle on the air-side heat transfer and pressure drop characteristics of a multi-louvered fin and flat tube heat exchanger has been examined experimentally. "A" and "V" shapes, and inclined one-slab air-cooled heat exchangers have been used in air-conditioning and heat pump applications for the cost-effective compact systems, although these configurations may deteriorate the system performance. There are some publications on the effect of an inclination angle on the heat transfer and the pressure drop of the heat exchangers. However, most of the published data have considered the bare-tube banks, high-fin tube banks and conventional finned tube heat exchangers [1–6].

Groehn [1] performed an experimental study on the effect of an inclination angle on the thermal hydraulic performance, using 28 bare-tube banks with different number of rows in both in-line and staggered arrangements. That study found that the heat transfer coefficients were not influenced by the inclination angle, while the pressure drops increased monotonically with the inclination angle in the lower Reynolds number range. They also reported that the pressure drops for the larger inclination angles ($\theta \geqslant 60°$) deviated more than those for the smaller inclination angles. Monheit and Freim [2] investigated experimentally the effect of an inclination angle on the performance of high-fin tube banks in close-packed staggered arrangements, and observed no effect of the inclination angle on the thermal performance. On the other hand, they reported that the pressure drops increased with the inclination angle for $\theta \geqslant 50°$, and that the effect was greater at the lower Reynolds number.

Moore and Ristorcelli [3] performed a theoretical study on the flow and pressure losses in a V-shaped region formed by oblique high-drag porous plates, which represented the downstream surfaces of the heat exchangers. They reported that the overall total pressure loss ascribable to the V configuration could be eliminated in principle by introduction of a uniform cascade of airfoils at the exit surface of each bundle, designed to

* Corresponding author. Tel.: +1-217-244-1531; fax: +1-217-333-1942.

E-mail address: mankim1@uiuc.edu (M.-H. Kim).

0017-9310/01/$ - see front matter © 2001 Published by Elsevier Science Ltd.
PII: S0017-9310(01)00104-1

Nomenclature

A_c	minimum free-flow area for air-side, m^2
A_f	fin surface area, m^2
A_{fr}	frontal area, m^2
A_o	total air-side surface area ($A_f + A_t$), m^2
A_t	external tube surface area, m^2
A_w	tube wall area, m^2
b'_i, b'_p, b_w	defined in Eq. (6)
c_p	specific heat, J/kg K
C_i	water-side capacity for wet surface, kg
C_o	air-side capacity for wet surface, kg
C_r	capacity ratio
D_h	hydraulic diameter, m
f	fanning friction factor
F_p	fin pitch, m
F_d	flow depth, m
H	fin height, m
h	heat transfer coefficient, W/m^2 K
i	enthalpy, kJ/kg
j	Colburn j-factor
k	thermal conductivity, W/m K
K_c	abrupt contraction coefficient
K_e	abrupt expansion coefficient
L	heat exchanger height, m
L_α	louver angle, °
L_l	louver length, m
L_p	louver pitch, m
$\dot{m}$	mass flow rate, kg/s
NTU	number of transfer units
Nu	Nusselt number (hD_h/k)
ΔP	pressure drop, Pa
Pr	Prandtl number (ν/α)
Q	heat transfer rate, W
Re_i	water-side Reynolds number ($V_i D_{hi}/\nu_i$)
Re_{L_p}	air-side Reynolds number based on louver pitch ($V_c L_p/\nu$)
t	temperature, °C
T_d	tube depth, m
u	face velocity, m/s
UA	overall transport coefficient, W/K (for dry condition) or kg/s (for wet condition)
V_c	maximum air velocity (uA_{fr}/A_c), m/s
V_i	water velocity, m/s
y	thickness of condensation water film, m

Greek symbols

α	thermal diffusivity ($k/\rho c_p$), m^2/s
β	constant for the correlation for f-factor
δ_f	fin thickness, m
δ_t	tube thickness, m
δ_w	tube wall thickness, m
ε	effectiveness
γ	aspect ratio of tube hole
η_f	fin efficiency
η_o	surface effectiveness
ν	viscosity, m^2/s
θ	inclination angle, °
ρ	density, kg/m^3
σ	contraction ratio of the fin array (A_c/A_{fr})

Subscripts

0	0° inclination angle
1	inlet
2	outlet
f	fin
i	water-side
duct	duct
m	mean value
max	maximum value
min	minimum value
n	nozzle
net	net value
o	air-side
P	tube surface
s	saturation state
t	tube
total	total
w	wet conditions or water
wall	tube wall

turn the flow immediately to the proper ultimate direction. Aarde and Kroger [4] determined experimentally the friction loss across an array of the A-frame finned tube heat exchangers. They derived flow loss correlations using scale model tests, and found that the downstream flow losses behind a V-bundle section were significantly influenced by the inclination angle, the process stream duct diameter, and the distance between the two-slab A-frames. Chang et al. [5] investigated the effect of inclination on the heat transfer and pressure drop characteristics for a forward-inclined wavy-finned circular tube heat exchanger. They found that both heat transfer coefficient and pressure drop decreased with increasing the inclination angle since the original staggered tube arrangement for $\theta = 0°$ changed to an in-line tube layout as the inclination angle increased.

Kedzierski [6] investigated experimentally the effect of inclination on the overall thermal hydraulic performance of a compact brazed plate heat exchanger using R-22 as a refrigerant and water as a heat transfer fluid. He found that a substantial performance penalty occurred for the evaporator due to stratification of refrigerant flow as the heat exchanger was tilted past 30° from the vertical. On the other hand, he reported that the overall heat transfer coefficient of the condenser improved by around 17–30% due to a thinner conden-

sate-film thickness as the heat exchanger was rotated to a horizontal position.

A microchannel tube heat exchanger is one of the potential alternatives for replacing the conventional finned tube heat exchangers and has been considered as both evaporator and gas cooler for prototype CO_2 air-conditioning systems [7]. Many investigators have studied the air-side heat transfer and the pressure drop characteristics of the louvered fin and flat tube heat exchangers [8–14]. Only one publication for the effect of inclination angle on the performance of the brazed aluminum heat exchangers is available in the open literature. Recently, Osada et al. [15] studied the effect of inclination on the heat transfer and pressure drop characteristics of corrugated multi-louvered fins, which are single-fin-row geometries with the larger flow depth (58, 70 mm) and fin spacing (3.0–4.0 mm). They reported that the leeward inclination improved fin performance. However, no published data are available in the open literature on the effect of an inclination angle on the thermal hydraulic performance of full scale brazed aluminum heat exchangers.

The purpose of this study is to provide experimental data on the effect of an inclination angle on the air-side thermal hydraulic performance for a multi-louvered fin and flat tube heat exchanger for both dry and wet conditions. A series of tests are conducted for the air-side Reynolds number range of 100–300 with variation of the inclination angles (0°, ±30°, ±45°, ±60° clockwise). The heat transfer and the friction loss coefficients are presented as a function of the Reynolds number, based on a louver pitch. Simple correlations are also presented, but will obviously need to be improved as more data become available for different geometries, and are combined with the data published here.

2. Experiments

2.1. Test apparatus

Fig. 1 shows a schematic diagram of the test apparatus used in the study. It consists of a suction-type wind tunnel, heat transfer fluid (water) circulation and control units, and data acquisition system. It is situated in a constant temperature and humidity chamber. The entrance of the wind tunnel is a rectangular duct 1240 mm wide and 935 mm high, where the test heat exchanger is installed. A stabilizing mesh is inserted at 400 mm downstream from the inlet of the wind tunnel to stabilize air flow induced through the heat exchanger. The air inlet conditions of the heat exchanger are maintained by controlling the chamber temperature and humidity. The inlet and outlet dry and wet bulb temperatures of the air are measured using the sampling units [16]. The air-side pressure drop through the heat exchanger is measured using a differential pressure transducer and the air flow rate is determined from the nozzle pressure difference. The heat transfer fluid circulation and control units maintain the water-side inlet condition by regulating the

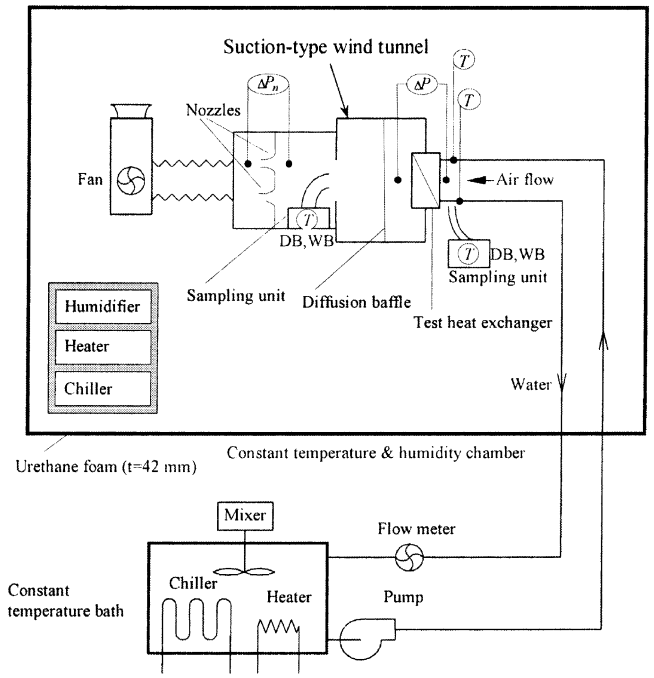

Fig. 1. Schematic diagram of test apparatus.

water flow rate and the inlet temperature. The uncertainty of heat transfer rate for the test apparatus is within ±3%, since accuracy of temperature measurement is ±0.1°C and accuracies of air and water flow rates are ±1% and ±2%, respectively.

2.2. Test heat exchanger

Figs. 2 and 3 indicate the geometrical configuration and the terminology of the test heat exchanger. The microchannel tube heat exchanger has louvered fins with 27°-louver angle, flow depth of 20 mm, fin pitch of 1.4 mm, and tube pitch of 10.05 mm. The louver pitch, louver length and fin height are 1.7, 6.4 and 8.15 mm, respectively, and the tested core size is 403 mm × 255 mm.

2.3. Test conditions and methods

The heat exchanger is installed at the wind tunnel entrance which is a rectangular duct 1240 mm × 940 mm, and insulation is placed around the heat exchanger to protect it from heat loss and air leakage as shown in Fig. 3. Table 1 shows the test conditions, including the inclination angles. For the inclination angles of $\theta = \pm 45°$, an upstream duct is also attached to investigate the effect of upstream turning on the performance of the heat exchanger. For both forward ($\theta = 0°$, 30°, 45°, 60° clockwise) and backward ($\theta = 0°$, −30°, −45°, −60° clockwise) inclinations a series of tests are performed in the range of Reynolds numbers 100–300, with water flow rate maintained at 0.32 m^3/h. The inlet air and water temperatures for the dry conditions are maintained at 21°C and 45°C, respectively. On the other hand, for the wet conditions, the inlet dry and wet bulb temperatures are 27°C and 19°C, respectively, and the water inlet temperatures are maintained at 6°C. The pressure drops were measured with (ΔP_{total}) and without (ΔP_{duct}) the heat exchanger installed to obtain the net pressure drops across the heat exchanger.

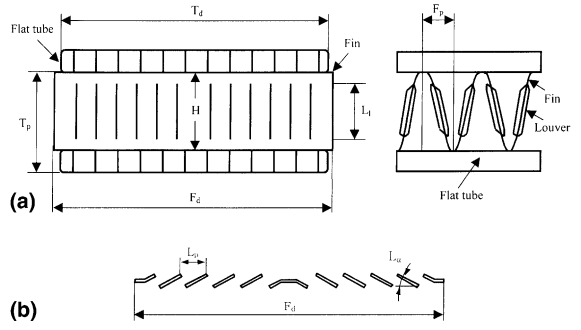

Fig. 2. Schematic of the test heat exchanger: (a) definition of geometric parameters; (b) cross-section of louvered fin geometry.

2.4. Data reduction

The data reduction process for the dry and wet conditions is the same as Kim and Bullard [11,12] used in their studies, so only a brief description is given here. The effectiveness–NTU method is used for obtaining the air-side heat transfer coefficient.

The ε–NTU equation for both fluid unmixed conditions is [17]

$$\varepsilon = 1 - \exp\left[\frac{\mathrm{NTU}^{0.22}}{C_r}\left\{\exp\left(-C_r \mathrm{NTU}^{0.78}\right) - 1\right\}\right]. \quad (1)$$

The effectiveness and NTU for both dry and wet conditions were determined using the arithmetic average of air- and water-side heat transfer rate (Q).

For dry surface:

$$\varepsilon = \frac{Q}{\dot{m}_o c_{p,o}(t_{i1} - t_{o1})},$$
$$\mathrm{NTU} = \frac{U_o A_o}{\left(\dot{m}c_p\right)_{min}}, \quad (2)$$
$$C_r = \frac{\left(\dot{m}c_p\right)_{min}}{\left(\dot{m}c_p\right)_{max}}.$$

For wet surface:

$$\varepsilon = \frac{Q}{\dot{m}_o(i_{o1} - i_{s,i1})},$$
$$\mathrm{NTU} = \frac{U_{ow} A_{ow}}{C_{min}}, \quad (3)$$
$$C_r = \frac{C_{min}}{C_{max}}, \quad C_o = \dot{m}_o, \quad C_i = \frac{m_i c_{p,i}}{b_i}$$

The air-side heat transfer coefficient can be obtained from the following equation.

For dry surface (based on temperature difference):

$$\frac{1}{U_o A_o} = \frac{1}{h_i A_i} + \frac{\delta_{wall}}{k_{wall} A_{wall}} + \frac{1}{\eta_o h_o A_o}. \quad (4)$$

For wet surface (based on enthalpy difference):

$$\frac{1}{U_{ow} A_{ow}} = \frac{b_i'}{h_i A_i} + \frac{b_P' \delta_{wall}}{k_{wall} A_{wall}} + \frac{b_w}{\eta_{ow} h_{ow} A_{ow}}, \quad (5)$$

$$b_i' = \frac{i_{s,Pi} - i_{s,i}}{t_{Pi} - t_i},$$
$$b_P' = \frac{i_{s,Po} - i_{s,Pi}}{t_{Po} - t_{Pi}}, \quad (6)$$
$$b_w = \frac{\Delta i_{s,w}}{\Delta t_{s,w}}.$$

For the heat transfer coefficients on the water-side, the following equation (with a rms error of ±3%) was developed based on earlier test results obtained using the same microchannel tubes used this study [11]:

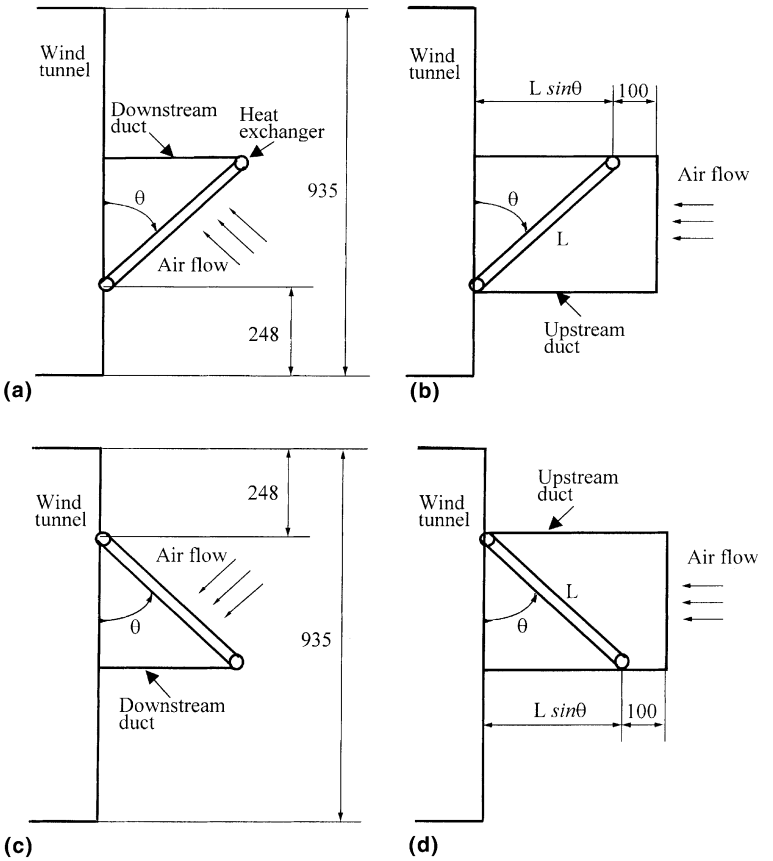

Fig. 3. Schematic diagram of heat exchanger installation for forward inclination ($\theta > 0°$) and backward inclination ($\theta < 0°$) [unit of length: mm]: (a) $\theta > 0°$ without upstream duct; (b) $\theta > 0°$ with upstream duct; (c) $\theta < 0°$ without upstream duct; (d) $\theta < 0°$ with upstream duct.

Table 1
Test conditions

	Air-side			Water-side		Inclination angle (clockwise, °)
	Flow rate (m^3/min)	Inlet temperature (°C)		Flow rate (m^3/h)	Inlet temperature (°C)	
		Dry bulb	Wet bulb			
Dry	4–12	21	16	0.32	45	0, ±30, ±45, ±60
Wet	4–12	27	19	0.32	6	

$$Nu_i = Nu_{\text{ref}} + 0.0499 Re_i Pr_i \frac{D_{\text{hi}}}{L},$$
$$Nu_{\text{ref}} = 7.541\left(1 - 1.969\gamma + 5.66\gamma^2 - 12.866\gamma^3 + 19.349\gamma^4 - 16.197\gamma^5 + 5.51\gamma^6\right). \quad (7)$$

The Nu_{ref} is derived using Schmidt's data cited by Shah and London [18] for the rectangular ducts of aspect ratio γ for the following boundary conditions: top and bottom walls isothermal and both sides adiabatic.

The surface effectiveness and the fin efficiency for the wet surface [19] are:

$$\eta_{\text{ow}} = 1 - \frac{A_{\text{f}}}{A_{\text{ow}}}(1 - \eta_{\text{fw}}), \quad (8)$$

$$\eta_{\text{fw}} = \frac{\tanh(m^* l)}{m^* l},$$

$$m^* = \sqrt{\frac{2h_{\text{ow}}}{k_{\text{f}}\delta_{\text{f}}}\left(1 + \frac{\delta_{\text{f}}}{F_{\text{d}}}\right)}, \quad (9)$$

$$l = H/2 - \delta_{\text{f}}.$$

The heat transfer coefficient for the wet surface is

$$h_{ow} = 1 \Big/ \left[\frac{c_{p,o}}{b_w h_o} + \frac{y_w}{k_w} \right], \tag{10}$$

where h_o is the sensible heat transfer coefficient for the wet surface, and y_w is the thickness of the condensation water film, which is assumed as 0.1 mm [20], even though the term y_w/k_w is usually negligible because it is very small compared to $c_{p,o}/(b_w h_o)$ in practice. For the dry conditions, the same equations for the fin and surface efficiencies can be used by replacing h_{ow} with h_o in Eq. (9).

The heat transfer coefficient and the pressure drop can be expressed as j- and f-factors

$$j = \frac{h_o}{\rho_m V_c c_{p,o}} Pr_o^{2/3}, \tag{11}$$

$$f = \frac{A_c}{A_o}\frac{\rho_m}{\rho_1}\left[\frac{2\rho_1 \Delta P}{(\rho_m V_c)^2} - (K_c + 1 - \sigma^2) - 2\left(\frac{\rho_1}{\rho_2} - 1\right) + (1 - \sigma^2 - K_e)\frac{\rho_1}{\rho_2} \right], \tag{12}$$

where K_c and K_e are the coefficients for pressure loss at the inlet and outlet of the heat exchanger [21]. Accounting for all instrument errors, uncertainties for the heat transfer coefficients and pressure drops were estimated to be ±12% and ±10%, respectively [22].

3. Results and discussion

Table 2 presents the measured heat transfer rates for both dry and wet conditions, compared to those of the referenced 0° inclination angle. The heat transfer rates for the same flow rate were not influenced significantly by either the upstream duct or the inclination angles. As shown in Table 2, the heat transfer rates for all the test conditions studied here are very similar and most (97%) of the data points are within 2% deviation from the 0° inclination angle.

Fig. 4 shows how the heat transfer coefficients vary with the inclination angle and the face velocity for both dry and wet conditions. As expected, heat transfer coefficients increased with the face velocity. The heat transfer coefficients for the dry conditions were not affected significantly by the inclination angles for $|\theta| \leqslant \pm 45°$, suggesting that the flow pattern through passages inside the heat exchanger remained generally louver-directed, with and without the upstream duct. However, the heat transfer coefficients deteriorated for the $\theta = \pm 60°$, where the exit turning angle was apparently large enough to disrupt flow over the downstream louvers as shown in Fig. 5. On the other hand, for the wet conditions the sensible heat transfer coefficients were influenced by the inclination angles. The heat transfer coefficients for $\theta > 0°$ decreased with inclination angle as the condensate had to drain by flowing against the air flow direction. However, for $\theta < 0°$ the heat transfer coefficient increased, because the air shear force enhanced condensate drainage. The sensible heat transfer coefficients for $\theta > 0°$ were 3–19% smaller than those for $\theta < 0°$ for $Re_{L_p} = 100$–300, respectively, reflecting the greater difference in condensate drainage patterns at higher Reynolds numbers.

The measured total pressure drops across the heat exchanger consist of the sum of the friction loss, the inlet and the exit losses, the downstream losses, and the upstream losses (when the upstream duct is present). The pressure drops through the duct were measured also before the heat exchanger was attached at the test section, and the net pressure drops across the heat exchanger were calculated as:

$$\Delta P_{net} = \Delta P_{total} - \Delta P_{duct}. \tag{13}$$

Table 3 shows the measured total and net pressure drop data for the dry conditions. The pressure drops in-

Table 2
Heat transfer data for both dry and wet conditions

Inclined angle, θ (°)	Air flow rate (m³/min)/heat transfer rate (W)									
	4 (m³/min)		6 (m³/min)		8 (m³/min)		10 (m³/min)		12 (m³/min)	
	Dry	Wet	Dry	Wet	Dry	Wet	Dry	Wet	Dry	Wet
−60	1499	1667	1990	2071	2366	2349	2681	2573	2946	2750
−45	1512	1643	2018	2086	2399	2373	2703	2577	2962	2774
−45*	1521	1654	2028	2048	2411	2336	2725	2540	2980	2710
−30	1536	1667	2037	2063	2422	2329	2710	2532	2959	2692
0	1513	1631	2029	2046	2419	2314	2733	2524	2995	2712
30	1538	1675	2039	2056	2449	2326	2778	2528	3031	2704
45	1522	1655	2026	2035	2426	2289	2746	2495	3004	2672
45*	1528	1653	2031	2032	2441	2292	2764	2510	3017	2691
60	1529	1654	2028	2015	2409	2273	2713	2467	2951	2616

* Data with the upstream duct.

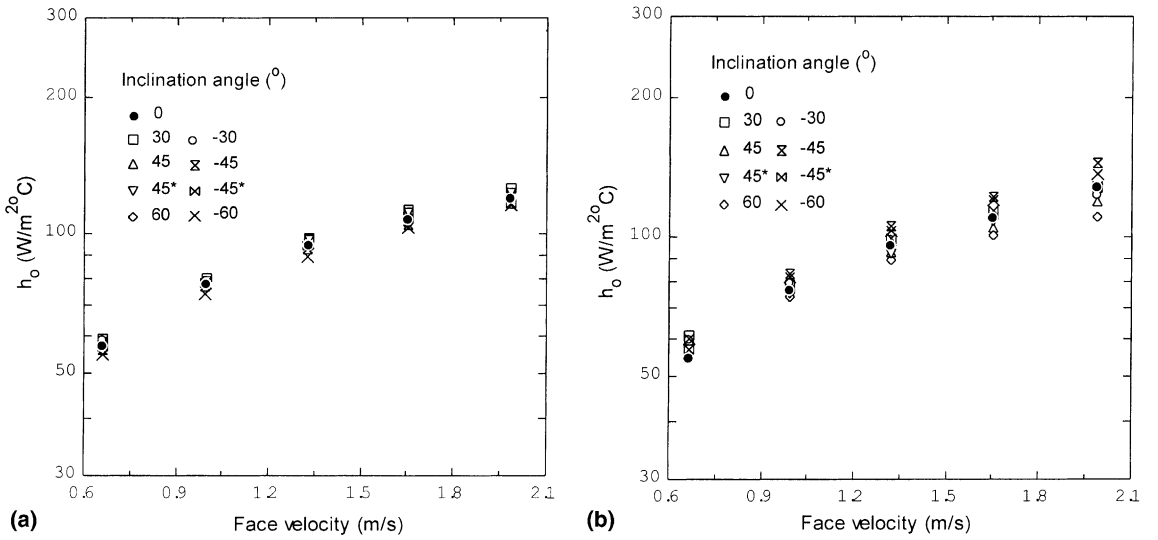

Fig. 4. Heat transfer coefficients vs. face velocity: (a) dry conditions; (b) wet conditions.

creased systematically with the inclination angles for both forward and backward inclinations. When the upstream duct was attached, the total and net pressure drops increased 4–11% and 6–14% for the $\theta = \pm 45°$, respectively. These may be due to the additional upstream losses associated with oblique entrance to the heat exchanger (the inlet flow is normal to the heat exchanger when the upstream duct is not present). The total and net pressure drops for $\theta > 0°$ were 1–13% and 1–16% larger, respectively, than those for $\theta < 0°$, reflecting the asymmetric exit losses associated with the louver geometry as shown in Fig. 5.

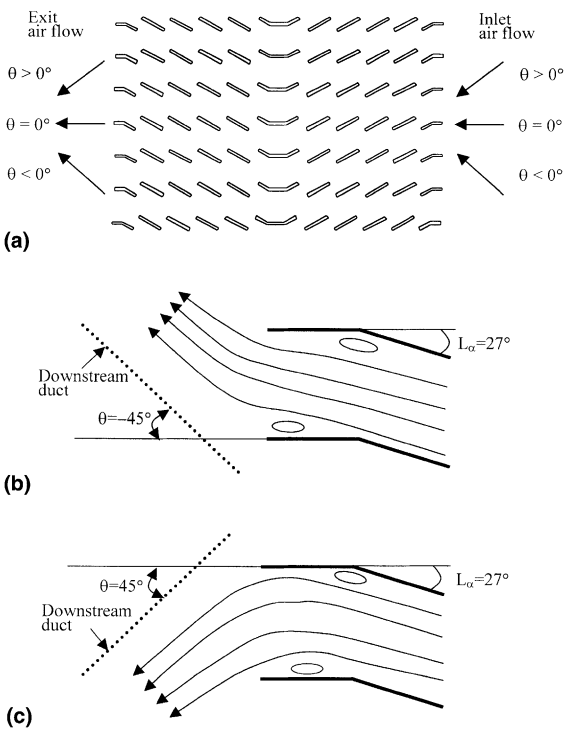

Fig. 5. Flow configuration of inlet and exit air flow: (a) inlet and exit air flow; (b) exit air flow for backward inclination ($\theta = -45°$); (c) exit air flow for forward inclination ($\theta = 45°$).

Table 4 presents the pressure drop data for the wet conditions. The general trends of the pressure drops for the wet conditions were similar to those for the dry conditions. For $\theta = \pm 45°$, the total and net pressure drops with the upstream duct were 1–12% larger than those for the case without the upstream duct. The ratios of the total and net pressure drops for $\theta > 0°$ and $\theta < 0°$ were 2–19% and 2–26%, respectively. The ratios increased with the flow rate since the condensate drain for $\theta > 0°$ was disturbed significantly by the air shear force as the flow rate increased, while for $\theta < 0°$ the air flow enhanced the condensate drainage. This result is similar to the heat transfer performance data, and indicates that the alignment of gravitational and air shear forces plays an important role in condensate drainage, which influences the thermal hydraulic performance of the heat exchanger. The inclination angle had a greater effect on the total pressure drop for both dry and wet conditions when the inclination angle exceeded 45°. However, such a big difference for the net pressure drops across the heat exchanger alone was not observed although the inclination angle was larger than 45°.

Figs. 6 and 7 present the j- and net f-factors for both dry and wet conditions as a function of the Reynolds number. As shown in the figures, the j-factors were similar for the same inclined direction and

Table 3
Pressure drop data for the dry conditions

Inclined angle, θ (°)	Air flow rate (m^3/min)/pressure drop (Pa)									
	4 (m^3/min)		6 (m^3/min)		8 (m^3/min)		10 (m^3/min)		12 (m^3/min)	
	ΔP_{total}	ΔP_{net}	ΔP_{total}	ΔP_{net}	ΔP_{total}	ΔP_{net}	ΔP_{total}	ΔP_{net}	ΔP_{total}	ΔP_{net}
−60	8.6	6.7	16.3	12.1	25.9	18.7	37.1	26.3	50.2	34.9
−45	7.6	6.6	13.2	11.2	20.3	17.0	28.0	22.9	36.7	29.5
−45*	8.0	7.0	14.3	12.3	21.8	18.5	30.4	25.2	40.7	33.6
−30	7.5	6.5	12.7	10.9	18.7	15.6	25.6	21.4	33.2	27.5
0	6.1	5.4	11.1	9.6	17.3	14.8	23.6	20.0	30.6	25.4
30	7.8	6.8	13.2	11.4	19.4	16.3	26.3	22.1	33.8	28.2
45	7.7	6.7	14.0	12.0	20.9	17.7	29.2	24.0	38.5	31.3
45*	8.3	7.3	14.8	12.9	22.9	19.6	31.9	26.7	42.5	35.3
60	9.7	7.7	18.1	13.8	28.6	21.4	40.3	29.5	54.3	38.9

* Data with the upstream duct.

Table 4
Pressure drop data for the wet conditions

Inclined angle, θ (°)	Air flow rate (m^3/min)/pressure drop (Pa)									
	4 (m^3/min)		6 (m^3/min)		8 (m^3/min)		10 (m^3/min)		12 (m^3/min)	
	ΔP_{total}	ΔP_{net}	ΔP_{total}	ΔP_{net}	ΔP_{total}	ΔP_{net}	ΔP_{total}	ΔP_{net}	ΔP_{total}	ΔP_{net}
−60	11.2	9.2	19.5	15.3	30.5	23.3	42.2	31.4	55.3	40.0
−45	8.8	7.8	15.5	13.5	23.6	20.4	32.5	27.3	40.7	33.6
−45*	9.3	8.3	17.0	15.0	26.0	22.8	35.4	30.2	44.4	37.3
−30	7.7	6.8	13.9	12.2	21.2	18.1	29.4	25.2	37.3	31.6
0	8.3	7.7	13.3	11.9	20.9	18.4	28.7	25.1	36.9	31.7
30	8.7	7.7	14.4	12.7	21.8	18.7	30.5	26.3	40.4	34.7
45	9.4	8.4	17.2	15.2	27.0	23.7	37.0	31.8	46.6	39.4
45*	9.5	8.5	17.7	15.7	28.3	25.0	39.3	34.1	51.1	43.9
60	11.4	9.4	21.5	17.3	33.9	26.8	48.4	37.6	65.8	50.5

* Data with the upstream duct.

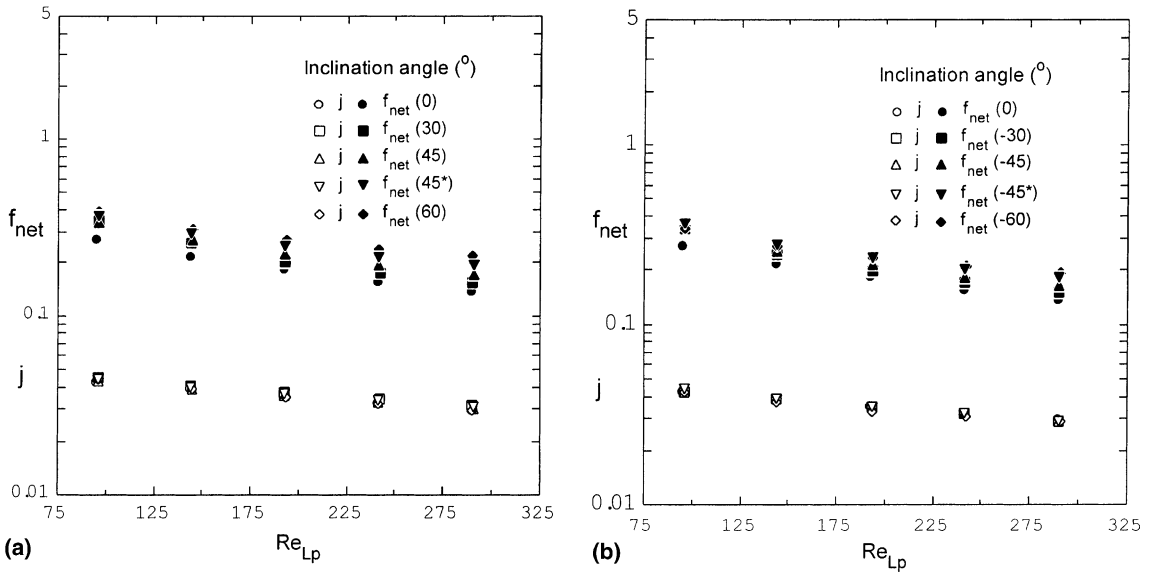

Fig. 6. *j*- and *f*-factors for dry conditions: (a) forward inclinations; (b) backward inclinations.

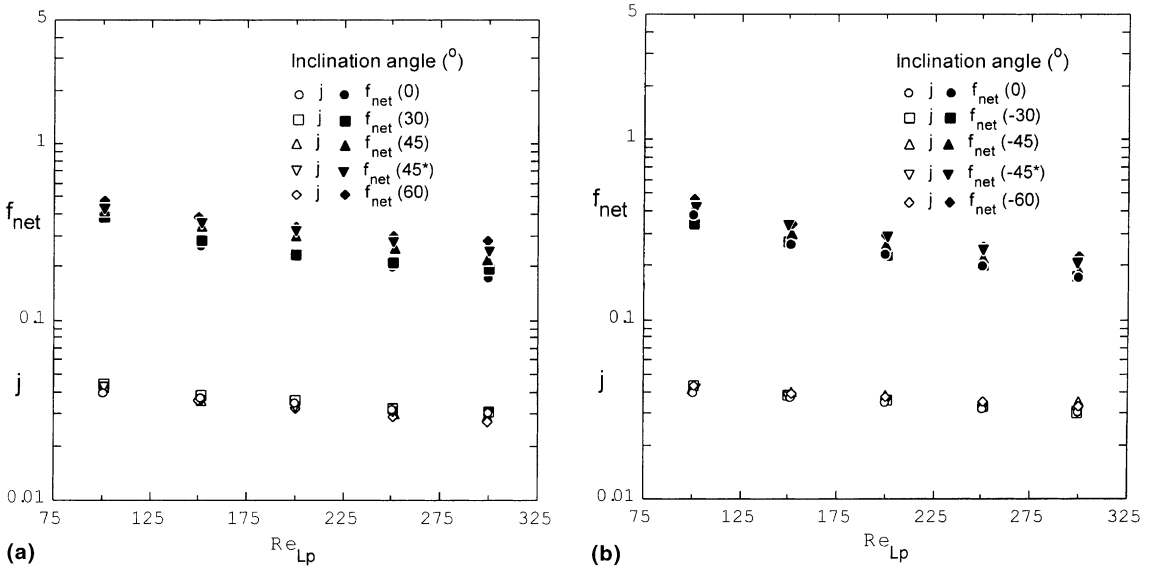

Fig. 7. *j*- and *f*-factors for wet conditions: (a) forward inclination; (b) backward inclination.

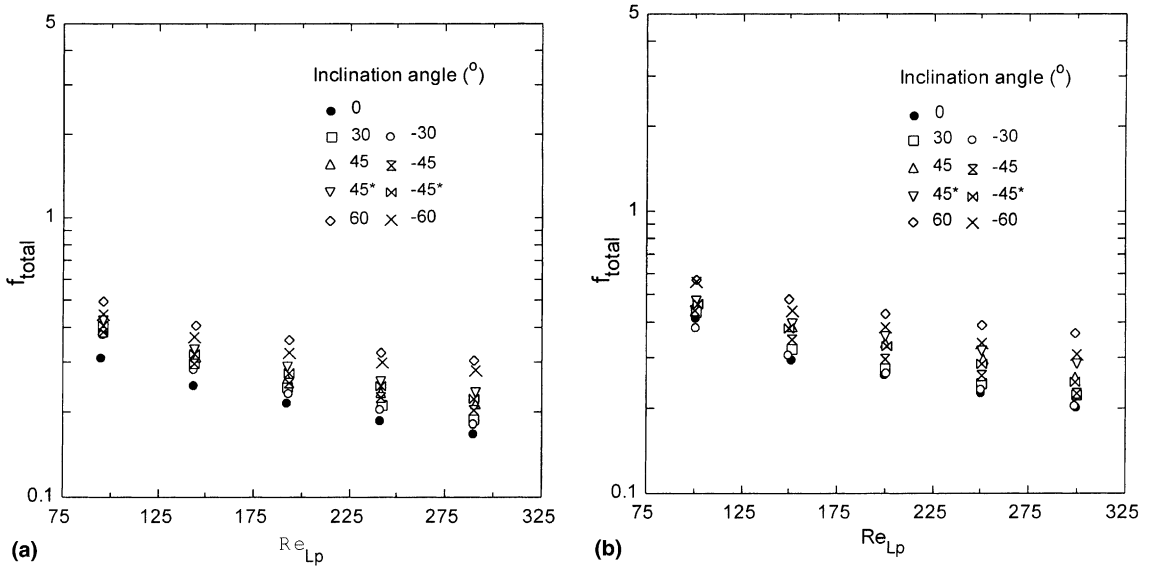

Fig. 8. *f*-factors for the total pressure drops: (a) dry conditions; (b) wet conditions.

surface (dry or wet) conditions studied here. The sensible *j*-factors for $\theta = 0°$ were about 90–101% of those for dry conditions, for the Reynolds numbers 100–300, similar to the findings of Kim and Bullard [11,12] for a larger Reynolds number range than that studied here. The net friction factors decreased with the Reynolds number, and increased with inclination angles as expected. The net *f*-factors for the wet conditions were 111–138% larger than those for the dry conditions, and varied with the Reynolds number, the angle and the direction of inclination as shown in Figs. 6 and 7.

Fig. 8 presents the *f*-factors for the total pressure drops for dry and wet conditions, respectively. The ratios of the f_{total} and f_{net} increased systematically with the inclination angle and the Reynolds number for both forward and backward inclinations. When the inclination angle was 0°, the values of f_{total} for the dry case were 13–22% larger than those of f_{net}, depending on the Reynolds number, while for the wet case they were

Table 5
Correlation constant (β) and rms errors for f-factors

Test condition	Inclined angle, θ (°)	f_{total}		f_{net}	
		β	Rms error (%)	β	Rms error (%)
Dry	$\theta \geqslant 0$	−0.453	±10.4	−0.172	±8.8
	$\theta \leqslant 0$	−0.373	±10.4	−0.069	±8.4
Wet	$\theta \geqslant 0$	−0.490	±11.8	−0.265	±8.2
	$\theta \leqslant 0$	−0.380	±10.8	−0.121	±7.3

9–17% larger. At $\theta = 60°$, the figures were 26–41% and 21–31% for the dry and wet conditions, respectively. For $\theta = -60°$, the figures were 30–46% and 22–39%, reflecting the increase of f_{net} due to the presence of condensate on fins. However, the ratios of f_{total} and f_{net} will depend on the duct configuration associated with the installation scheme of the heat exchanger, which affect the upstream and downstream flows.

When the upstream duct was not present, the following correlations for both dry and wet conditions were derived, based on the referenced 0° inclination angle's correlations (f_0) [11,12]:

$$f_\theta = f_0\left(1 - \frac{|\theta|}{90}\right)^\beta, \tag{14}$$

where

$$f_0 = Re_{L_p}^{-0.781}\left(\frac{L_\alpha}{90}\right)^{0.444}\left(\frac{F_p}{L_p}\right)^{-1.682}\left(\frac{H}{L_p}\right)^{-1.22} \times \left(\frac{F_d}{L_p}\right)^{0.818}\left(\frac{L_l}{L_p}\right)^{1.97} \text{ for dry conditions,} \tag{15}$$

$$f_0 = Re_{L_p}^{-0.798}\left(\frac{L_\alpha}{90}\right)^{0.395}\left(\frac{F_p}{L_p}\right)^{-2.635}\left(\frac{H}{L_p}\right)^{-1.22} \times \left(\frac{F_d}{L_p}\right)^{0.823}\left(\frac{L_l}{L_p}\right)^{1.97} \text{ for wet conditions.} \tag{16}$$

Table 5 presents correlation constant (β) and rms errors for both f_{total} and f_{net}, showing that the correlations fit well experimental data for the geometry studied here. Their applicability to the different louvered-fin geometries needs to be confirmed by additional experiments, especially for higher inclination angles $\theta \approx 90°$-louver angle where the exit air flow could be nearly parallel or normal to the louvers, as shown in Fig. 5.

4. Concluding remarks

The effect of forward and backward inclinations on the heat transfer coefficients and pressure drops of a multi-louvered fin heat exchanger for both dry and wet conditions has been investigated experimentally. The wind tunnel geometry simulated air flow patterns typical of evaporators in wall-mounted mini-split systems, where air enters normal to the coil and is then turned through a duct. The following conclusions obtained:

1. Heat transfer characteristics for both dry and wet conditions were neither significantly affected by the inclination angle ($-60° < \theta < 60°$), nor by the presence or absence of an upstream duct.
2. The sensible heat transfer coefficients and pressure drops for wet conditions were influenced significantly by the air shear force of air flow at high Reynolds number, especially in case of large inclination angles, and the gravitational force played an important role in condensate drainage.
3. The net and total pressure drops increased consistently with inclination angles.
4. The total pressure drops for the forward inclination were larger than those of the backward inclination, reflecting the asymmetry associated the louver geometry.
5. The friction factor correlations for both total and net (heat exchanger only) pressure drops were developed, based on the 0° inclination angle's f-factors within rms errors ±10.4% and ±8.8% for dry conditions and ±11.8% and ±8.2% for wet conditions, respectively.
6. When the upstream duct was present, the pressure drops were 7–16% larger than those for the case of absence of the upstream duct, due to the additional turn required for the air to flow through the folded fins of the microchannel heat exchanger.

Acknowledgements

We are grateful to Samsung Electronics Co., Hydro Aluminum A.S., and The Trane Company for supporting this study.

References

[1] H.G. Groehn, Heat transfer and flow resistance of yawed tube bundle heat exchangers, Heat Exchanger: Theory and Practice, Hemisphere, Washington, DC, 1983, pp. 299–310.

[2] M. Monheit, J. Freim, Effect of tube bank inclination on the thermal hydraulic performance of air cooled heat exchangers, in: Proc. 8th Int. Heat Transfer Conference, 1986, pp. 2727–2732.
[3] F.K. Moore, J.R. Ristorcelli, Turbulent flow and pressure drop losses behind oblique high-drag heat exchangers, Int. J. Heat Mass Transfer 22 (1979) 1175–1186.
[4] D.J. Aarde, D.G. Kroger, Flow losses through an array of A-frame heat exchangers, Heat Transfer Eng. 14 (1) (1993) 43–51.
[5] W.R. Chang, C.-C. Wang, Y.J. Chang, Effect of an inclination angle on the heat transfer and pressure drop characteristics of a wavy finned-tube heat exchanger, ASHRAE Trans. 100 (Pt. 2) (1994) 826–832.
[6] M.A. Kedzierski, Effect of inclination on the performance of a compact brazed plate condenser and evaporator, Heat Transfer Eng. 18 (3) (1997) 25–38.
[7] M.-H. Kim, J.M. Yin, C.W. Bullard, P.S. Hrnjak, Development of a micro-channel evaporator model for a CO_2 mobile air-conditioner, in: Proceedings of the ASME, Advanced Energy Systems Division-2000, vol. 40, 2000, pp. 47–54.
[8] A. Sahnoun, R.L. Webb, Prediction of heat transfer and friction for the louver fin geometry, J. Heat Transfer 114 (1992) 893–900.
[9] Y. Chang, C. Wang, Air side performance of brazed aluminum heat exchangers, J. Enhanced Heat Transfer 3 (1) (1996) 15–28.
[10] Y. Chang, C. Wang, A generalized heat transfer correlation for louvered fin geometry, Int. J. Heat Mass Transfer 40 (3) (1997) 533–544.
[11] M.-H. Kim, C.W. Bullard, Air-side thermal hydraulic performance of multi-louvered fin aluminum heat exchangers, Int. J. Refrig., 2001, in press.
[12] M.-H. Kim, C.W. Bullard, Air-side thermal performance of micro-channel heat exchangers under dehumidifying conditions, in: Proceedings of the International Refrigeration Conference at Purdue, 2000, pp. 119–126.
[13] W.J. McLaughlin, R.L. Webb, Wet air side performance of louver fin automotive evaporators, SAE Technical Paper Series, 2000-01-0574, 2000.
[14] W.J. McLaughlin, R.L. Webb, Condensate drainage and retention in louver fin automotive evaporators, SAE Technical Paper Series, 2000-01-0574, 2000.
[15] H. Osada, H. Aoki, T. Ohara, Kuroyanagi, Experimental analysis for enhancing automotive evaporator fin performance, in: R.K. Shah (Ed.), Proceedings of the International Conference on Compact Heat Exchangers and Enhancement Technology for the Process Industries, 1999, pp. 439–445.
[16] ANSI/ASHRAE Standard 41.1-1986, Standard Method for Temperature Measurement, ASHRAE, Atlanta, Georgia, 1986.
[17] F.P. Incropera, D.P. DeWitt, Fundamentals of Heat and Mass Transfer, third ed., Wiley, New York, 1990.
[18] R.K. Shah, A.L. London, Laminar Flow Forced Convection in Ducts – A Source Book for Compact Heat Exchanger Analytical Data, Academic Press, New York, 1978.
[19] T.H. Kuehn, J.W. Ramsey, J.L. Threlkeld, Thermal Environmental Engineering, third ed., Prentice-Hall, Englewood Cliffs, NJ, 1998, pp. 289–331.
[20] R.J. Myers, The effect of dehumidification on the air-side heat transfer coefficient for a finned tube coil, M.S. Thesis, University of Minnesota, Minneapolis, 1967.
[21] W.M. Kays, A.L. London, Compact Heat Exchangers, third ed., McGraw-Hill, New York, 1984.
[22] R.J. Moffat, Describing the uncertainties in experimental results, Exp. Thermal Fluid Sci. 1 (1988) 3–17.